CRYSTAL GROWTH & DESIGN

pubs.acs.org/crystal

Article

Two Hydrogen-Bonded Organic Frameworks with Imidazole Encapsulation: Synthesis and Proton Conductivity

Biao-Biao Hao, Xin-Xin Wang, Chen-Xi Zhang,* and Qinglun Wang*

Cite This: *Cryst. Growth Des.* 2021, 21, 3908−3915

Read Online

ACCESS | Metrics & More | Article Recommendations | Supporting Information

ABSTRACT: On the basis of the carboxylic structure of trimesic acid (TMA) and 5-borono-1,3-benzenedicarboxylic acid (B-BDC), here two hydrogen-bonded organic frameworks (HOFs), HOF **1** (MA-TMA) and HOF **2** (MA-B-BDC), were prepared by reacting melamine (MA) with trimesic acid and 5-borono-1,3-benzenedicarboxylic acid, respectively. The as-prepared HOF **1** and HOF **2** with 3D supramolecular structure exhibit excellent performance in proton transport. AC impedance test shows that the proton conductivities of HOF **1** and HOF **2** reach 3.11×10^{-4} S·cm^{-1} (343 K, 98% RH) and 4.32×10^{-4} S·cm^{-1} (323 K, 98% RH), respectively. To increase the proton conductivity, Im@HOF **1** and Im@HOF **2** were obtained by introducing imidazole (Im), which acts as a jumping site for proton transfer. The proton conductivities of Im@HOF **1** and Im@HOF **2** reached 4.12×10^{-4} S·cm^{-1} (333 K, 98% RH) and 1.20×10^{-3} S·cm^{-1} (353 K, 98% RH), respectively. This is the first time that guest molecules were introduced into HOFs. The stability and proton conductivity of the HOFs are improved due to the interaction of imidazole with carboxyl groups and water molecules.

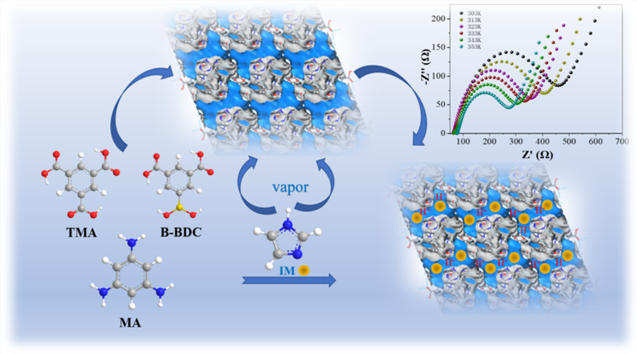

1. INTRODUCTION

With the development of science and technology, emphasis on environmental improvement becomes increasingly crucial.[1] Fuel cells can directly convert chemical energy into electric energy with the characteristics of high conversion rate and no pollution, which has a great prospect of development and application in many aspects.[2−5] Proton-exchange membrane (PEM) is an important part of proton-exchange fuel cells,[6,7] as it isolates the filling fuel at the poles, thereby affecting the transport of electrons. An excellent PEM can maintain a good proton conduction path so that protons can reach the cathode through the membrane and react to release energy. Good stability and efficient proton conduction ability are necessary for proton-exchange membranes. Therefore, the study of proton-exchange membrane is of great significance.[8] For example, Nafion membranes have excellent proton conductivities;[9−11] however, water loss at high temperatures leads to a sharp decrease in conductivity. Moreover, high synthesis cost would limit the application of Nafion membranes in fuel cells. Since then, low-cost aromatic polymers have been widely studied as alternatives to perfluorinated sulfonic acid proton-exchange membranes.[12,13] However, films of this type are prone to swell under high humidity and are unstable under high temperatures. To solve the problems of costs and stabilities, metal−organic frameworks (MOFs), covalent organic frameworks (COFs), and hydrogen-bonded organic frameworks (HOFs) are used and discovered with great significance to proton conductivity.[14−18]

Compared with MOFs and COFs, HOFs are formed through the interaction of hydrogen-bonding forces.[19−23] HOFs have high proton conductivity but poor stability for the weak hydrogen bonds.[24−26] Therefore, this shortcoming limits their use under high-temperature conditions. Selective introduction of guest molecules[27,28] can increase the number of hydrogen bonds and the stabilities of HOFs.[29−31] The large number of hydrogen-bond networks inside HOFs play a key role in the stability of the structure and proton conduction.[32−37] Therefore, it is particularly important to improve the proton conduction characteristics and stabilities of these materials.[38−44]

Here, two types of HOFs are synthesized through the reaction of melamine with trimesic acid and 5-borono-1,3-benzenedicarboxylic acid, respectively. To increase proton conductivity, Im@HOF **1** and Im@HOF **2** were obtained by introducing imidazole through vapor diffusion.[45,46] It is found that Im@HOF **2** achieved a high proton conduction performance of 1.20×10^{-3} S·cm^{-1} (353 K, 98% RH), which is nearly 3 times higher than that of HOF **2**. This

Received: February 23, 2021
Revised: May 27, 2021
Published: June 4, 2021

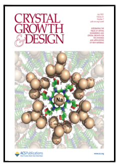

https://doi.org/10.1021/acs.cgd.1c00214
Cryst. Growth Des. 2021, 21, 3908−3915

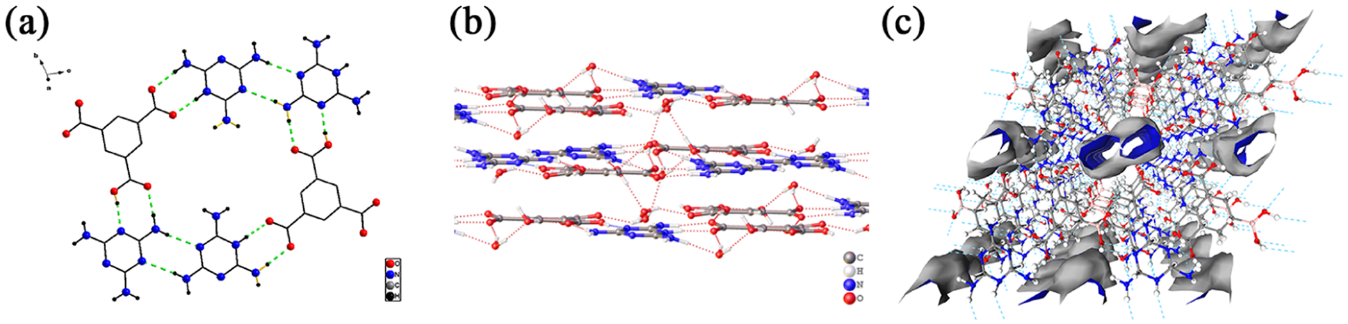

Figure 1. (a) Unit of network structure in the plane, (b) layered structures connected by hydrogen bonds, and (c) 3D structure of HOF **1** with holes.

method of doping HOFs is first proposed here and will have great significance for future work.

2. EXPERIMENTAL SECTION

2.1. Materials. Melamine (purity 99%) was purchased from Aladdin Company. Trimesic acid (98%) was purchased from Aladdin Company. Imidazole (99%) was purchased from Shanghai Bi De Pharmaceutical Technology Company.

2.2. Synthesis of 5-Borono-1,3-benzenedicarboxylic Acid. 5-Borono-1,3-benzenedicarboxylic acid was synthesized according to the method in the previous article, with slight modifications.[47] A quantity of 1.05 g (7.14 mmol) of 3,5-dimethylphenylboronic acid and 0.5184 g (14.48 mmol) of NaOH were dissolved in 100 mL of deionized water/*tert*-butanol solution (v/v = 1:1) and heated to 40 °C before 0.5 g of potassium permanganate was added. When the color of the solution faded, 6.83 g of potassium permanganate was added seven times, and the solution was mixed well and heated to 50 °C for 3 h. Once the color of the solution turned brown, the solution was filtered and the residue was rinsed with hot water. The obtained filtrate was concentrated to 20 mL under vacuum and acidified by adding concentrated hydrochloric acid to pH = 1. 5-Borono-1,3-benzenedicarboxylic acid was thus obtained as a white solid and washed with a lot of water and then dried in a vacuum environment. Yield: 1.01 g, 69.1%. ^{1}H NMR ($CDCl_3$): δ (ppm) 8.39 (br s, 2H), 8.53 (s, 1H), 8.59 (s, 2H), 13.32 (br s, 2H).

2.3. Preparation of HOF 1 and HOF 2. HOF **1** was synthesized according to the literature.[48,49] Melamine (0.063 g, 0.5 mmol) and trimesic acid (0.105 g, 0.5 mmol) were placed in a 100 mL round-bottom flask, separately. A volume of 50 mL of deionized water was added, and the two solutions were stirred for 0.5 h at 70 °C. After cooling down to room temperature, the two solutions were mixed together and stirred for 1 h. The white blocky substance called HOF **1** was obtained by filtering and washing with deionized water. Finally, HOF **1** was dried under vacuum at 50 °C. In the same way, using 5-borono-1,3-benzenedicarboxylic acid instead of trimesic acid, the blocky substance HOF **2** was obtained. Elemental Anal. Calcd for HOF **1** $C_{12}H_{18}N_6O_{19}$: C, 26.1%; H, 3.2%; N 15.2%; Found: C, 26.3%; H, 3.8%; N, 16.2%; Calcd for HOF **2** $C_{11}H_{19}N_6O_{19}B$: C, 24.0%; H, 3.4%; N, 15.2%; Found: C, 23.7%; H, 3.6%; N, 15.5%; FTIR (KBr, cm^{-1}) for HOF **1**: 3390 (s), 3243 (m), 1740 (m), 1658 (m), 1280 (s), 759 (m), 686 (m); HOF **2**: 3339 (m), 1652 (m), 1618 (w), 1553 (m), 775 (s), 714 (m), 577 (m).

2.4. Preparation of Im@HOF 1 and Im@HOF 2. A quantity of 0.6 g of HOF **1** was placed in a 50 mL beaker, which was placed in a sealed container containing 5 g of imidazole powder. The container was heated at a temperature of 120 °C for 72 h in a vacuum oven and a slightly yellowish product of Im@HOF **1** was formed. Using the same method, the corresponding Im@HOF **2** was formed by replacing HOF **1** with HOF **2**. Elemental Anal. Found for Im@HOF **1**: C, 43.9%; N, 25.6%; H, 4.8% (yield = 60% based on N); Im@HOF **2**: C, 42.1%; N, 23.4%; H, 4.1% (yield = 44% based on N); FTIR (KBr, cm^{-1}) for Im@HOF **1**: 3357 (s), 3119 (m), 3036 (m), 2847 (m), 1677 (s), 1348 (m), 1153 (m), 1083 (m), 859 (m), 733 (m); Im@HOF **2**: 3357 (m), 3334 (m), 3132 (s), 2844 (m), 1650 (s), 1371 (m), 1190 (m), 1027 (m), 815 (m), 703 (m).

2.5. Characterization of FTIR, PXRD, and N_2 Adsorption. A sheet made up of the sample and KBr was used to carry out Fourier transform infrared (FTIR) spectroscopy study (Bruker Tensor 27). At 293 K, a Bruker D8 instrument was used to record X-ray powder diffraction patterns on the synthesized material in the 2θ angle range of 5−50°. The nitrogen adsorption test was carried out with Autosorb-IQ-MP (Quantachrome) at −196 °C.

2.6. Proton Conduction Measurement. The obtained HOFs were ground into powder and compressed by a tablet machine to obtain small disks with a thickness of about 0.5 mm. Both sides of the disk were evenly coated with carbon conductive glue and fixed with electrodes in a sealed environment with different humidities. Humidity was controlled by different saturated salt solutions of $NaNO_2$ (65% RH), NaCl (75% RH), KCl (86% RH), KNO_3 (93% RH), and K_2SO_4 (98% RH). The materials were kept for 24 h under the corresponding humidity before the AC impedance test. The calculation formula is as follows

$$\sigma = d/SR$$

Here, σ is the proton conductivity (S·cm^{-1}), d is the thickness of the sheet (cm), S is the surface area of the sheet (cm^2), and R is the resistance of the sheet (Ω).

The corresponding activation energy can be calculated by testing the proton conductivity at different temperatures and humidities, which can be used to discuss and study the mechanism of proton conduction. The specific Arrhenius equation is as follows

$$\sigma_T = \sigma_0 \exp(-E_a/k_B T)$$

where σ_0 is the prereference factor, E_a is the activation energy, and k_B is the Boltzmann constant.

3. RESULTS AND DISCUSSION

3.1. Structural Characterizations. Since trimesic acid and melamine are acidic and basic compounds, respectively, it is easy to form a large number of hydrogen bonds in HOF **1**, which increases the stability of the HOFs.[50] According to the previous reports,[47] its hydrogen bond structure is shown in Figure 1. Based on HOF **1**,[47] the structure of HOF **2** is obtained by changing a carboxyl group in trimesic acid to a boronic acid group using Materials Studio 8.0.[51] There are four different types of hydrogen bonds (Figure 1a) that constitute the network framework of HOF **1** and HOF **2**.[48,52] A plane unit of HOF **1** is formed by four melamine and two trimesic acid molecules through hydrogen bonding (Figure 1a). Two hydrogen bonds can be formed by an amino group from melamine in the cavity and two water molecules. One-dimensional chains of hydrogen bonds are formed by adjacent water molecules in pores, which provide support for the multilayer network structure of HOF **1**. In addition, the $\pi-\pi$

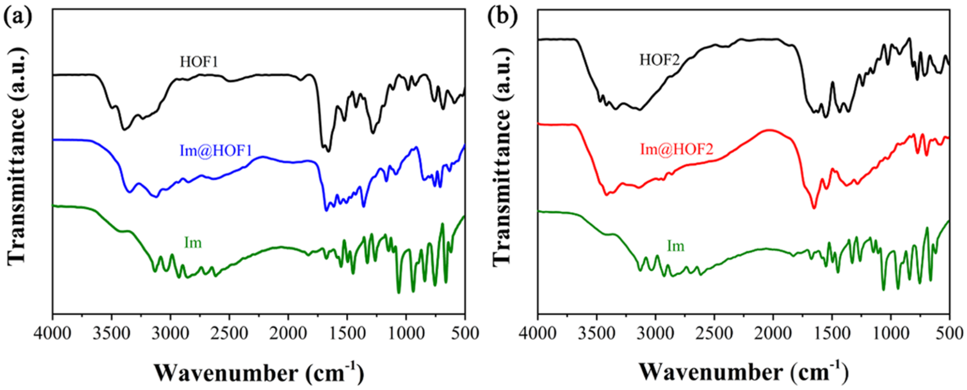

Figure 2. (a) Infrared absorption spectra of HOF **1** (black), Im (green), and Im@HOF **1** (blue). (b) Infrared absorption spectra of HOF **2** (black), Im (green), and Im@HOF **2** (red).

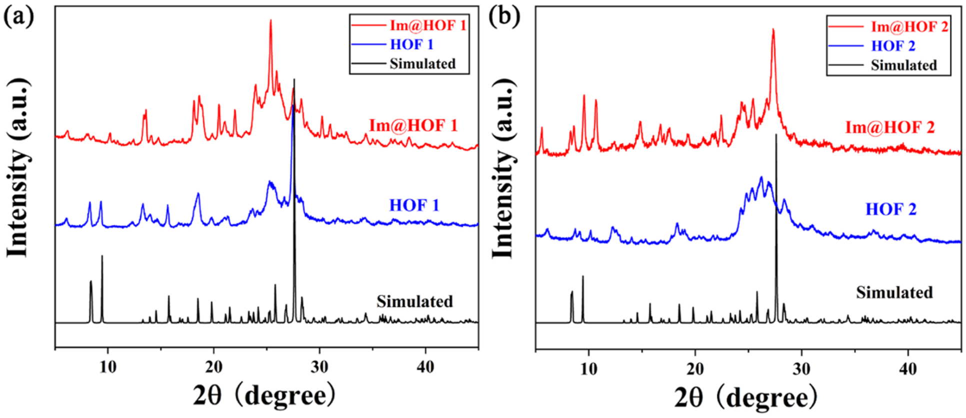

Figure 3. PXRD spectra of (a) HOF **1** and (b) HOF **2** for simulated, as-synthesized, and imidazole doping.

stacking between melamine and trimesic acid also plays an important role in stabilizing the layered structure of HOF **1** (Figure 1b). In the angle of view perpendicular to the plane layer, HOF **1** can be seen as a 3D structure with holes (Figure 1c). Compared with HOF **1**, the network structure of HOF **2** is not changed except that the boronic acid group has one more hydroxyl than the carboxyl group, which can form more hydrogen bonds with water molecules (Figure S1). Hydrogen bonds can also be formed by the water molecules in the pores and amino groups from melamine, which provide many proton conduction pathways.

3.2. Infrared (IR) Absorption Spectrum. The characteristic absorption wavelengths that occurred at 2848 and 2604 cm^{-1} belong to imidazole molecules. After being doped with imidazole, both Im@HOF **1** and Im@HOF **2** show the characteristic absorption peaks of imidazole molecules in Figure 2a,b, which indicates that imidazole is successfully incorporated into the two HOFs.

3.3. TGA and PXRD Patterns. The thermal properties of HOF **1** and HOF **2** are shown in Figure S2. The weight of HOF **1** reduces by 5.5% under 95 °C and decreases rapidly by about 70% under 380 °C. The first weight loss is attributed to the loss of water molecules in the voids of HOF **1**, and the second large-scale mass loss is attributed to the collapse of the HOF **1** framework. After imidazole doping, Im@HOF **1** has a mass loss of 10% at about 180 °C, which proves that Im@HOF **1** has better thermal stability than HOF **1**. The higher weight loss of water molecules proves that the introduction of imidazole increases the adsorption of water molecules by HOF **1**, which is attributed to the formation of hydrogen bonds between water molecules and N−H of the imidazole structure. Compared with HOF **1**, twice weight losses of HOF **2** and Im@HOF **2** both occur at 100−150 and 340 °C, respectively (Figure S2). It is worth noting that Im@HOF **2** has relatively higher stability because of its smaller weight loss in the range of 100−150 °C, which indirectly proves that the introduction of imidazole molecules will enhance the stability of HOF **2**. The electron-withdrawing ability of carboxylic acids is stronger than that of boric acids, which makes its conversion to CO_2 easier at high temperatures, leading to weight losses of 90.9% and 71.4 % for Im@HOF **1** and Im@HOF **2** at 500 K, respectively.

The PXRD spectra of HOF **1** and HOF **2** are compared with the previous report.[49] As shown in Figure 3, the structures of HOF **1** and HOF **2** maintain good stability before and after imidazole vapor diffusion, which can be clearly seen from the PXRD spectrum (Figure 3a,b). The PXRD spectra of Im@HOF **1** and Im@HOF **2** were analyzed by immersing them in water at 100 °C and testing their conductivity 5 times. The result shows that they are stable under high-temperature and high-humidity conditions (Figure S3).

3.4. Nitrogen Adsorption Properties. Before the nitrogen adsorption test, HOF **1** and HOF **2** were placed in a vacuum drying oven at 100 °C for 24 h for activation. Nitrogen adsorption study reveals that the highest nitrogen adsorption capacities of HOF **1** and HOF **2** are 117 and 62 $cm^3 \cdot g^{-1}$ and the specific surface areas are 10.99 and 6.13 $m^2 \cdot g^{-1}$, respectively. From the adsorption and desorption curves, it is found that both HOF **1** and HOF **2** belong to the type III

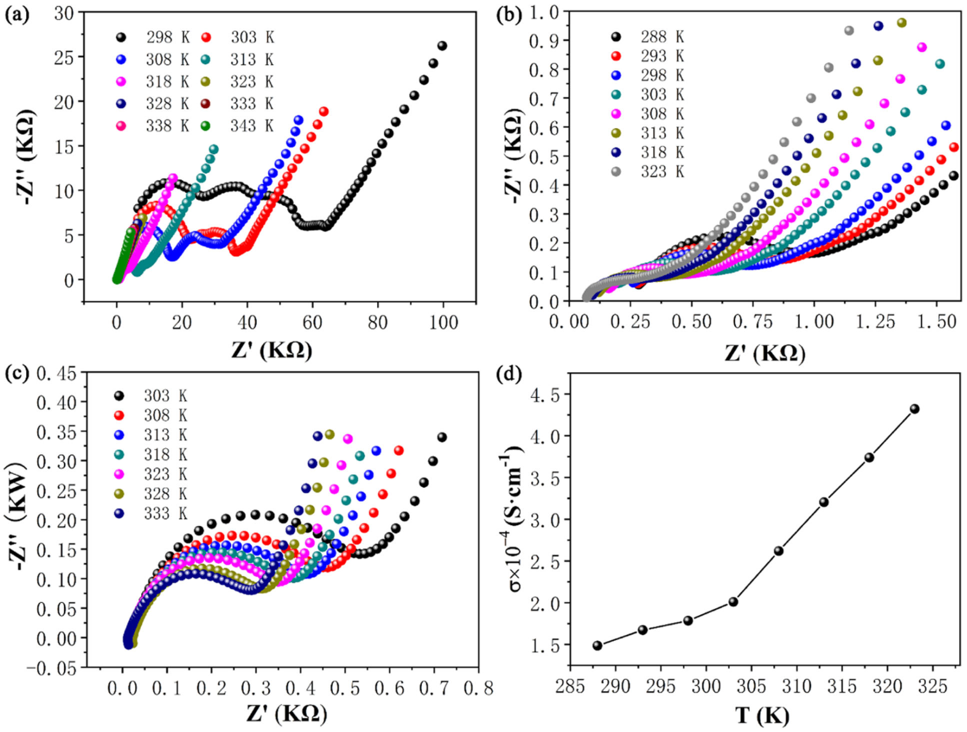

Figure 4. (a) AC impedance spectrum of HOF **1** at 98% RH and 298−343 K. (b) AC impedance spectrum of Im@HOF **1** under 98% RH and 288−323 K. (c) AC impedance spectrum of HOF **2** at 98% RH and 303−333 K. (d) Proton conductivity of Im@HOF **1** at 98% RH at 298−323 K.

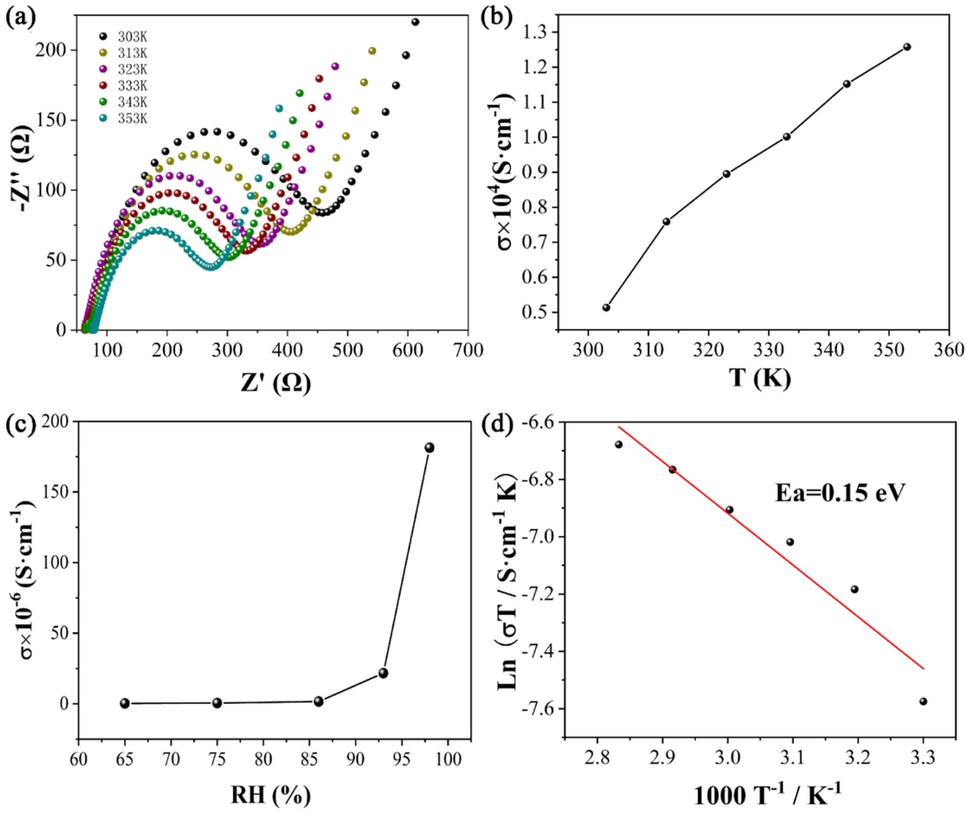

Figure 5. (a) AC impedance spectrum of Im@HOF **2** at 98% RH and 303−353 K. (b) Proton conductivity of Im@HOF **2** at 98% RH and 303−353 K. (c) Proton conductivity of Im@HOF **2** at room temperature and 65−98% RH. (d) E_a of Im@HOF **2** at 98% RH and 303−353 K.

adsorption (Figure S4), which reveals that the interaction force between HOFs and nitrogen is relatively weak.[26,53] As expected, the amount of nitrogen adsorbed by Im@HOF **1** and Im@HOF **2** dropped significantly after the introduction of imidazole molecules. The nitrogen adsorption capacities of Im@HOF **1** and Im@HOF **2** are only 10 and 12 $cm^3 \cdot g^{-1}$, respectively, which definitely proves that imidazole has entered the pores of the material.

3.5. Proton Conductivity Properties.

Organic molecular structures with amino and carboxyl groups are often used to develop proton-conducting materials at high humidities. HOF **1** and HOF **2** have good proton conductivity owing to their structures, which feature a large number of carboxyl groups and an extensive network of hydrogen bonds. The high proton conductivity of HOF **1** and HOF **2** is verified by the AC impedance test.

Figures 4a, S5, and S6 display the measurement of the proton conductivity of HOF **1** at different humidities and temperatures. The Nernst curve of HOF **1** shows that as the relative humidity increases from 65% RH to 98% RH at room temperature, the proton conductivity of HOF **1** increases from 1.20×10^{-8} $S \cdot cm^{-1}$ (298 K, 65% RH) to 4.80×10^{-6} $S \cdot cm^{-1}$ (298 K, 98% RH). This clearly indicates that water plays a significant role in the proton conduction pathway. In HOF **2**, the boronic acid group has one more hydroxyl than the carboxyl group so that it can form hydrogen bonds with more water molecules, resulting in a higher proton conductivity than HOF **1**. Under the condition of 298 K, the proton conductivity of HOF **2** also increases from 1.04×10^{-7} $S \cdot cm^{-1}$ (298 K, 65% RH) to 1.64×10^{-4} $S \cdot cm^{-1}$ (298 K, 98% RH) when the environmental humidity steadily increased (Figure 5c).

With the increase of temperature under humidity at 98%, the highest proton conductivities of HOF **1** and HOF **2** are 3.11×10^{-4} $S \cdot cm^{-1}$ (343 K, 98% RH) and 4.32×10^{-4} $S \cdot cm^{-1}$ (323 K, 98% RH), respectively (Figures 4a and S5). Such high proton conductivity mainly depends on the interaction of a large number of internal hydrogen bond network frameworks and water molecules.

In addition, many previous works involved imidazole doped in membranes and MOFs have been reported to improve the conductivity of protons.[16−18] There are two scientific arguments: one holds that the rotation of the central axis of the imidazole molecule transfers protons, and the other is that the conjugated hydrogen bonds in the molecule accelerate H^+ transmission.[7,8,15] Considering that the 1D hydrogen bond chains are formed by the water molecules and amino groups from melamine in the cavities, the role of imidazole in our work should be a rotary carrier belonging to the first argument. Im@HOF **1** and Im@HOF **2** are obtained through the vapor diffusion method, and the AC impedance test is performed (Figures 4b and 5a). The proton conductivity of Im@HOF **1** increases from 2.09×10^{-4} $S \cdot cm^{-1}$ (303 K, 98% RH) to 4.12×10^{-4} $S \cdot cm^{-1}$ (333 K, 98% RH) in the temperature range of 298 to 333 K under 98% relative humidity (Figure 4d). As expected, Im@HOF **1** also shows an upward trend in its proton conductivity as the temperature increases. The proton conductivity of Im@HOF **1**, i.e., 2.09×10^{-4} $S \cdot cm^{-1}$ (303 K, 98% RH), is 2 orders of magnitude higher than the proton conductivity of HOF **1**, i.e., 4.80×10^{-6} $S \cdot cm^{-1}$ (298 K, 98% RH) of HOF **1** (Figure S5), which indicates that imidazole is successfully doped to receive and deliver protons (Figure 6). The E_a values of HOF **1** are 0.50 eV (298−313 K) and 0.71 eV (313−338 K), while that of Im@HOF **1** is 0.28 eV (Figure S7), which indicates that imidazole provides a proton jumping site during proton conduction and the mechanism of proton conduction changes from the vehicle mechanism to the Grotthuss mechanism.

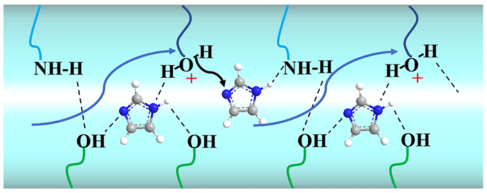

Figure 6. Protons transferred by imidazole in pore species.

Im@HOF **2** has the highest proton conductivity of 1.20×10^{-3} $S \cdot cm^{-1}$ at 98% relative humidity and 353 K, which is about 3 times higher than the proton conductivity of HOF **2** before doping with imidazole (Figure 5a,b), proving that proton conductivity is successfully improved by the introduction of imidazole. The proton conductivity of Im@HOF **2** reaches a maximum of 4.32×10^{-4} $S \cdot cm^{-1}$ when the relative humidity is 98% at room temperature (Figure 5c). The E_a values of HOF **2** and Im@HOF **2** are 0.39 and 0.15 eV, respectively, which also show that the participation of imidazole reduces the energy required for proton transport (Figures 5d and S7). It also proves that the proton transfer mechanisms of HOF **2** and Im@HOF **2** are all Grotthuss mechanisms. As shown in Table 1, compared with the HOFs reported in the literature,[41−44] the synthesized Im@HOF **2** exhibits relatively high proton conductivity.

Table 1. Summary of Proton Conductivities ($S \cdot cm^{-1}$) for HOFs

HOF	network structure	σ ($S \cdot cm^{-1}$)	E_a (eV)	ref
HOF-6a	3D	3.4×10^{-6}	_	37
HOF-GS-10	2D	7.5×10^{-3}	0.489	38
HOF-GS-11	2D	1.8×10^{-2}	0.135	38
CPOS-1	3D	1.0×10^{-2}	0.93	39
CPOS-2	3D	2.2×10^{-2}	0.61	39
CPOS-3	3D	3.3×10^{-4}	0.62	39
CPOS-4	3D	7.4×10^{-4}	0.82	39
HOF-H_3L	3D	6.91×10^{-5}	0.68	40
HOF **1**	3D	3.11×10^{-4}	0.50,[a] 0.71[b]	this work
Im@HOF **1**	3D	4.12×10^{-4}	0.28	this work
HOF **2**	3D	4.32×10^{-4}	0.39	this work
Im@HOF **2**	3D	1.20×10^{-3}	0.15	this work

[a] For T = 298−313 K. [b] For T = 313−338 K.

3.6. Proton Conduction Mechanism.

Proton transfer in proton conductive materials has been extensively studied, including two proton transfer pathways, which are determined by the activation energy (E_a). When E_a > 0.4 eV, it is considered to be the vehicle mechanism, and when E_a < 0.4 eV, it is considered to be the Grotthuss mechanism. According to the vehicle mechanism, the proton is carried to the destination by a single carrier, whereas the Grotthuss mechanism indicates that the proton is transmitted to each other by the cooperation of multiple carriers.[54,55] As shown in Figure 6, a large number of pores in HOF **1** and HOF **2** are filled by imidazole molecules. The one-dimensional proton hydrogen bond channels are formed by the interaction of imidazole with hydroxyl and amino groups from water and melamine molecules (Figure S8), respectively. Protons can be received by imidazole molecules and then transferred to form protonated water molecules through hydrogen bonding, maintaining the transmission of protons. The activation energies of HOF **1** and HOF **2** are 0.50 (298−313 K)/0.71 (at 313−338 K) and 0.39 eV, while the activation energies of Im@HOF **1** and Im@HOF **2** are 0.28 and 0.15 eV at 98% relative humidity, respectively, which fully demonstrate that imidazole acts as a proton carrier and reduces the energy required for migration in the process.[56−58]

4. CONCLUSIONS

In summary, we have successfully synthesized two HOFs that have high proton conductivity. Moreover, the imidazole was successfully introduced into the pores of these two HOFs through the vapor diffusion method to further improve the proton conductivity. Finally, the proton conductivity of Im@HOF **1** and Im@HOF **2** reached the highest values of 4.12×10^{-4} S·cm^{-1} (333 K, 98% RH) and 1.20×10^{-3} S·cm^{-1} (333 K, 98% RH), respectively. The study shows that imidazole has a very significant promotion effect on proton conductivity. The strategy of doping HOFs was used for the first time to improve the proton conductivity of HOFs, which has a guiding significance for the doping and modification of HOFs in the future.

■ ASSOCIATED CONTENT

Supporting Information

The Supporting Information is available free of charge at https://pubs.acs.org/doi/10.1021/acs.cgd.1c00214.

Structure of HOF 2; TGA images; comparison of proton conduction values; comparison of E_a; nitrogen adsorption isotherms; and structure of 1D chain formed by water molecules through hydrogen bonds (PDF)

■ AUTHOR INFORMATION

Corresponding Authors

Chen-Xi Zhang − *College of Chemical Engineering and Materials Science, Tianjin University of Science and Technology, Tianjin 300457, P. R. China; Key Laboratory of Brine Chemical Engineering and Resource Eco-utilization, Tianjin University of Science and Technology, Tianjin 300457, P. R. China;* orcid.org/0000-0003-3383-9112; Email: zcx@tust.edu.cn

Qinglun Wang − *College of Chemistry, Nankai University, Tianjin 300071, P. R. China; Key Laboratory of Advanced Energy Materials Chemistry (Ministry of Education), Nankai University, Tianjin 300071, P. R. China;* orcid.org/0000-0002-0983-6280; Email: wangql@nankai.edu.cn

Authors

Biao-Biao Hao − *College of Chemical Engineering and Materials Science, Tianjin University of Science and Technology, Tianjin 300457, P. R. China*

Xin-Xin Wang − *College of Chemical Engineering and Materials Science, Tianjin University of Science and Technology, Tianjin 300457, P. R. China*

Complete contact information is available at: https://pubs.acs.org/10.1021/acs.cgd.1c00214

Author Contributions

All authors contributed to the discussion and writing of the manuscript. The final version was approved by all authors.

Notes

The authors declare no competing financial interest.

■ ACKNOWLEDGMENTS

This work was supported by the National Natural Science Foundation of China (Nos. 21771111, 21371104, 20771081, 21101096, and 21471084) and Tianjin Research Innovation Project for Postgraduate Students (2020YJSS051).

■ REFERENCES

(1) Ye, Y.; Gong, L.; Xiang, S.; Zhang, Z.; Chen, B. Metal-Organic Frameworks as a Versatile Platform for Proton Conductors. *Adv. Mater.* **2020**, *32*, No. 1907090.

(2) Lin, R. B.; He, Y.; Li, P.; Wang, H.; Zhou, W.; Chen, B. Multifunctional porous hydrogen-bonded organic framework materials. *Chem. Soc. Rev.* **2019**, *48*, 1362−1389.

(3) Xie, X.; Yang, Y.; Dou, B.; Li, Z.; Li, G. Proton conductive carboxylate-based metal−organic frameworks. *Coord. Chem. Rev.* **2020**, *403*, No. 213100.

(4) Liu, S.; Zhao, Y.; Zhang, C.; Lin, L.; Li, Y.; Song, Y. The novel excited state intramolecular proton transfer broken by intermolecular hydrogen bonds in HOF system. *Spectrochim. Acta, Part A* **2019**, *219*, 164−172.

(5) Chen, B. An ultrastable and easily regenerated HOF for the selective storage and separation of light hydrocarbons. *Sci. China: Chem.* **2017**, *60*, 683−684.

(6) Guo, L.; Sun, J.; Wei, J.; Liu, Y.; Hou, L.; Yuan, C. Conductive metal-organic frameworks: Recent advances in electrochemical energy-related applications and perspectives. *Carbon Energy* **2020**, *2*, 203−222.

(7) Yang, F.; Xu, G.; Dou, Y.; Wang, B.; Zhang, H.; Wu, H.; Zhou, W.; Li, J.; Chen, B. A flexible metal−organic framework with a high density of sulfonic acid sites for proton conduction. *Nat. Energy* **2017**, *2*, 877−883.

(8) Deng, X.; Hu, J.; Luo, J.; Liao, W.; He, J. Conductive Metal-Organic Frameworks: Mechanisms, Design Strategies and Recent Advances. *Top. Curr. Chem.* **2020**, *378*, No. 27.

(9) Han, J.; Lee, H.; Kim, J.; Kim, S.; Kim, H.; Kim, E.; Sung, Y.; Kim, K.; Lee, J. Sulfonated poly(arylene ether sulfone) composite membrane having sulfonated polytriazole grafted graphene oxide for high-performance proton exchange membrane fuel cells. *J. Membr. Sci.* **2020**, *612*, No. 118428.

(10) Sun, S.; Ling, L.; Xiong, Y.; Zhang, Y.; Li, Z. Trifluoromethanesulfonimide-based hygroscopic semi-interpenetrating polymer network for enhanced proton conductivity of nafion-based proton exchange membranes at low humidity. *J. Membr. Sci.* **2020**, *612*, No. 118339.

(11) Lutful Kabir, M. D.; Paul, S.; Choi, S.; Kim, H. Improved Electrochemical and Mechanical Properties of Poly(vinylpyrrolidone)/Nafion (R) Membrane for Fuel Cell Applications. *J. Nanosci. Nanotechnol.* **2020**, *20*, 7793−7799.

(12) Lu, P.; Shang, D.; Yang, C.; Sun, Y. An organic synaptic transistor with Nafion electrolyte. *J. Phys. D: Appl. Phys.* **2020**, *53*, No. 485102.

(13) Yang, X.; Zhu, H.; Jiang, F.; Zhou, X. Notably enhanced proton conductivity by thermally-induced phase-separation transition of Nafion/ Poly(vinylidene fluoride) blend membranes. *J. Power Sources* **2020**, *473*, No. 228586.

(14) Okawa, H.; Otsubo, K.; Yoshida, Y.; Kitagawa, H. Remarkably enhanced proton conduction of $\{NBu_2(CH_2COOH)_2\}$ $MnCr(ox)_3)$ by multiplication of carboxyl carrier in the cation. *Chem. Commun.* **2020**, *56*, 6138−6140.

(15) Xie, X.; Zhang, Z.; Zhang, J.; Hou, L.; Li, Z.; Li, G. Impressive Proton Conductivities of Two Highly Stable Metal-Organic Frameworks Constructed by Substituted Imidazoledicarboxylates. *Inorg. Chem.* **2019**, *58*, 5173−5182.

(16) Chen, L.; Pu, Z.; Long, Y.; Tang, H.; Liu, X. Synthesis and Properties of Sulfonated Poly(arylene ether nitrile) Copolymers Containing Carboxyl Groups for Proton- Exchange Membrane Materials. *J. Appl. Polym. Sci.* **2014**, *131*, 742−751.

(17) Okawa, H.; Sadakiyo, M.; Yamada, T.; Maesato, M.; Ohba, M.; Kitagawa, H. Proton-Conductive Magnetic Metal-Organic Frameworks, $\{NR_3(CH_2COOH)\}$ (MaMbIII)-M-II$(ox)_3$): Effect of Carboxyl Residue upon Proton Conduction. *J. Am. Chem. Soc.* **2013**, *135*, 2256−2262.

(18) Sun, P.; Wang, Y.; Li, Z.; Wang, C.; Pei, H.; Yin, X. Organic-inorganic backbone with high contents of proton conducting groups: A newly designed high performance proton conductor. *Int. J. Hydrogen Energy* **2020**, *45*, 14407−14412.

(19) Castells-Gil, J.; Padial, N.; Martí-Gastaldo, C. Structural reorganization in a hydrogen-bonded organic framework. *New J. Chem.* **2018**, *42*, 16138−16143.

(20) Han, Y.; Yuan, Y.; Wang, H. B. Porous Hydrogen-Bonded Organic Frameworks. *Molecules* **2017**, *22*, No. 266.

(21) Lu, T.; Ma, K.; Zhao, C.; Gu, Y.; Su, H.; Li, R. Solvothermal synthesis, crystal structure and properties of a new bisphosphonic-trimesic acid adduct. *J. Iran. Chem. Soc.* **2015**, *12*, 1183−1189.

(22) Peng, Y.; Gan, Y.; Shi, R.; Huang, W.; Tao, T. Construction of a Layered Hydrogen-Bonded Organic Framework Showing High-Contrast Mechanoresponsive Luminescence Turn-On. *J. Phys. Chem. C* **2018**, *122*, 29488−29497.

(23) Guo, Z.; Shi, Z.; Wang, X.; Li, Z.; Li, G. Proton conductive covalent organic frameworks. *Coord. Chem. Rev.* **2020**, *422*, No. 213465.

(24) Korolkov, V.; Allen, S.; Roberts, C.; Tendler, S. Green Chemistry Approach to Surface Decoration: Trimesic Acid Self-Assembly on HOPG. *J. Phys. Chem. C* **2012**, *116*, 11519−11525.

(25) Ibenskas, A.; Šimėnas, M.; Kizlaitis, K.; Tornau, E. Trimesic Acid Molecule in a Hexagonal Pore: Central versus Noncentral Position. *J. Phys. Chem. C* **2019**, *123*, 3552−3559.

(26) Zhou, H.; Ye, Q.; Wu, X.; Song, J.; Cho, C.; Zong, Y.; Tang, B.; Hor, T.; Yeow, E.; Xu, J. A thermally stable and reversible microporous hydrogen-bonded organic framework: aggregation induced emission and metal ion-sensing properties. *J. Mater. Chem. C* **2015**, *3*, 11874−11880.

(27) Wang, Y.; Liu, D.; Yin, J.; Shang, Y.; Du, J.; Kang, Z.; Wang, R.; Chen, Y.; Sun, D.; Jiang, J. An ultrafast responsive NO_2 gas sensor based on a hydrogen-bonded organic framework material. *Chem. Commun.* **2020**, *56*, 703−706.

(28) Yan, W.; Yu, X.; Yan, T.; Wu, D.; Ning, E.; Qi, Y.; Han, Y.; Li, Q. A triptycene-based porous hydrogen-bonded organic framework for guest incorporation with tailored fitting. *Chem. Commun.* **2017**, *53*, 3677−3680.

(29) Luo, Y.; He, X.; Hong, D.; Chen, C.; Chen, F.; Jiao, J.; Zhai, L.; Guo, L.; Sun, B. A Dynamic 3D Hydrogen-Bonded Organic Frameworks with Highly Water Affinity. *Adv. Funct. Mater.* **2018**, *28*, No. 1804822.

(30) Cai, S.; Shi, H.; Zhang, Z.; Wang, X.; Ma, H.; Gan, N.; Wu, Q.; Cheng, Z.; Ling, K.; Gu, M.; Ma, C.; Gu, L.; An, Z.; Huang, W. Hydrogen-Bonded Organic Aromatic Frameworks for Ultralong Phosphorescence by Intralayer pi-pi Interactions. *Angew. Chem., Int. Ed.* **2018**, *57*, 4005−4009.

(31) Feng, S.; Shang, Y.; Wang, Z.; Kang, Z.; Wang, R.; Jiang, J.; Fan, L.; Fan, W.; Liu, Z.; Kong, G.; Feng, Y.; Hu, S.; Guo, H.; Sun, D. Fabrication of a Hydrogen-Bonded Organic Framework Membrane through Solution Processing for Pressure-Regulated Gas Separation. *Angew. Chem., Int. Ed.* **2020**, *59*, 3840−3845.

(32) Liu, S.; Zhao, Y.; Zhang, C.; Lin, L.; Li, Y.; Song, Y. The novel excited state intramolecular proton transfer broken by intermolecular hydrogen bonds in HOF system. *Spectrochim. Acta, Part A* **2019**, *219*, 164−172.

(33) Karmakar, A.; Illathvalappil, R.; Anothumakkool, B.; Sen, A.; Samanta, P.; Desai, A.; Kurungot, S.; Ghosh, S. Hydrogen-Bonded Organic Frameworks (HOFs): A New Class of Porous Crystalline Proton-Conducting Materials. *Angew. Chem., Int. Ed.* **2016**, *55*, 10667−10671.

(34) Yang, J.; Wang, J.; Hou, B.; Huang, X.; Wang, T.; Bao, Y.; Hao, H. Porous hydrogen-bonded organic frameworks (HOFs): From design to potential applications. *Chem. Eng. J.* **2020**, *399*, No. 125873.

(35) Macdonald, J.; Dorrestein, P.; Pilley, M. Design of supramolecular layers via self-assembly of imidazole and carboxylic acids. *Cryst. Growth Des.* **2001**, *1*, 29−38.

(36) Pogorzelec-Glaser, K.; Pawlaczyk, C.; Pietraszko, A.; Markiewicz, E. Crystal structure and electrical conductivity of imidazolium succinate. *J. Power Sources* **2007**, *173*, 800−805.

(37) Awniczak, P.; Pogorzelec-Glaser, K.; Pietraszko, A.; Hilczer, B. Impedance spectroscopy studies of proton conductivity in imidazolium malonate. *Solid State Ionics* **2017**, *306*, 25−30.

(38) Hisaki, I. Hydrogen-bonded porous frameworks constructed by rigid pi-conjugated molecules with carboxy groups. *J. Inclusion Phenom. Macrocyclic Chem.* **2020**, *96*, 215−231.

(39) Hisaki, I.; Suzuki, Y.; Gomez, E.; Ji, Q.; Tohnai, N.; Nakamura, T.; Douhal, A. Acid Responsive Hydrogen-Bonded Organic Frameworks. *J. Am. Chem. Soc.* **2019**, *141*, 2111−2121.

(40) Hisaki, I.; Chen, X.; Takahashi, K.; Nakamura, T. Designing Hydrogen-Bonded Organic Frameworks (HOFs) with Permanent Porosity. *Angew. Chem., Int. Ed.* **2019**, *58*, 14794.

(41) Yang, W.; Yang, F.; Hu, T.; King, S.; Wang, H.; Wu, H.; Zhou, W.; Li, J.; Arman, H.; Chen, B. Microporous Diaminotriazine-Decorated Porphyrin-Based Hydrogen-Bonded Organic Framework: Permanent Porosity and Proton Conduction. *Cryst. Growth Des.* **2016**, *16*, 5831−5835.

(42) Karmakar, A.; llathvalappil, R.; Anothumakkool, B.; Sen, A.; Samanta, P.; Desai, A.; Kurungot, S.; Ghosh, S. Hydrogen-Bonded Organic Frameworks (HOFs): A New Class of Porous Crystalline Proton-Conducting Materials. *Angew. Chem., Int. Ed.* **2016**, *55*, 10667−10671.

(43) Xing, G.; Yan, T.; Das, S.; Teng, B.; Qiu, S. Synthesis of Crystalline Porous Organic Salts with High Proton Conductivity. *Angew. Chem., Int. Ed.* **2018**, *130*, 5443−5447.

(44) Sun, Z.; Li, Y.; Zhang, Z.; Li, Z.; Xiao, B.; Li, G. A path to improve proton conductivity: from a 3D hydrogen-bonded organic framework to a 3D copper-organic framework. *New J. Chem.* **2019**, *43*, 10637−10644.

(45) Shimizu, G.; Hurd, J.; Vaidhyanathan, R.; Thangadurai, V.; Ratcliffe, C.; Moudrakovski, I. Anhydrous proton conduction at 150°c in a crystalline metal-organic framework. *Nat. Chem.* **2009**, *1*, 705−710.

(46) Umeyama, D.; Horike, S.; Inukai, M.; Hijikata, Y.; Kitagawa, S. Confinement of mobile histamine in coordination nanochannels for fast proton transfer. *Angew. Chem., Int. Ed.* **2011**, *50*, 11706−11709.

(47) Lin, X.; Telepeni, I.; Blake, A.; Dailly, A.; Brown, C.; Simmons, J.; Zoppi, M.; Walker, G.; Thomas, K.; Mays, T.; Hubberstey, P.; Champness, N.; Schroeder, M. High Capacity Hydrogen Adsorption in Cu(II) Tetracarboxylate Framework Materials: The Role of Pore Size, Ligand Functionalization, and Exposed Metal Sites. *J. Am. Chem. Soc.* **2009**, *131*, 2159−2171.

(48) Li, B.; Bai, C.; Zhang, S.; Zhao, X.; Li, Y.; Wang, L.; Ding, K.; Shu, X.; Li, S.; Ma, L. An adaptive supramolecular organic framework for highly efficient separation of uranium via an in situ induced fit mechanism. *J. Mater. Chem. A* **2015**, 3, 23788−23798.

(49) Zhang, X.; Chen, X. Supramolecular Architectures and Helical Water Chains in Cocrystals of Melamine and Aromatic Carboxylic Acids. *Cryst. Growth Des.* **2005**, *5*, 617−622.

(50) Cullen, D.; Gardiner, M.; White, N. A three dimensional hydrogen bonded organic framework assembled through antielectrostatic hydrogen bonds. *Chem. Commun.* **2019**, *55*, 12020−12023.

(51) Jiang, S.; Gan, S.; Zhang, X.; Li, H.; Qi, Q.; Cui, F.; Lu, J.; Zhao, X. Aminal-Linked Covalent Organic Frameworks through Condensation of Secondary Amine with Aldehyde. *J. Am. Chem. Soc.* **2019**, *141*, 14981−14986.

(52) Almeida Paz, F.; Klinowski, J. Supramolecular architecture of a novel salt of trimesic acid and 1,2-bis(4-pyridyl)ethane. *CrystEngComm* **2003**, *5*, 238−244.

(53) Tang, Y.; Yuan, M.; Jiang, B.; Xiao, Y.; Fu, Y.; Chen, S.; Deng, Z.; Pan, Q.; Tian, C.; Fu, H. Inorganic acid-derived hydrogen-bonded organic frameworks to form nitrogen-rich carbon nitrides for

photocatalytic hydrogen evolution. *J. Mater. Chem. A* **2017**, *5*, 21979−21985.

(54) Cukierman, S. Et tu, Grotthuss! and other unfinished stories. *Biochim. Biophys. Acta, Bioenerg.* **2006**, *1757*, 876−885.

(55) Shi, L.; Ying, Z.; Xu, A.; Cheng, Y. Unraveling the water-mediated proton conduction mechanism along the surface of graphene oxide. *Chem. Mater.* **2020**, *32*, 6062−6069.

(56) Hori, Y.; Chikai, T.; Ida, T.; Mizuno, M. Local structure and hydrogen bond characteristics of imidazole molecules for proton conduction in acid and base proton-conducting composite materials. *Phys. Chem. Chem. Phys.* **2018**, *20*, 10311−10318.

(57) Hori, Y.; Suetake, T.; Shiota, Y.; Yoshizawa, K.; Shigeta, Y.; Ida, T.; Mizuno, M. Local Structures and Dynamics of Imidazole Molecules in Poly(vinylphosphonic acid)−Imidazole Composite Investigated by Molecular Dynamics. *ACS Appl. Polym. Mater.* **2020**, *2*, 1561−1568.

(58) Kumar, A.; Pisula, W.; Müllen, K. Effect of humidity and temperature on proton conduction in phosphonated copolymers. *Mater. Today Commun.* **2019**, *20*, No. 100539.